

Implications for first-order cosmological phase transitions and the formation of primordial black holes from the third LIGO-Virgo observing run

A. Romero²

K. Martinovic, T. A. Callister, H. Guo, M. Martínez, O. Pujolas,
M. Sakellariadou, V. Vaskonen, F. Yang and Y. Zhao

²Institut de Física d'Altes Energies (IFAE), The Barcelona Institute of Science and Technology

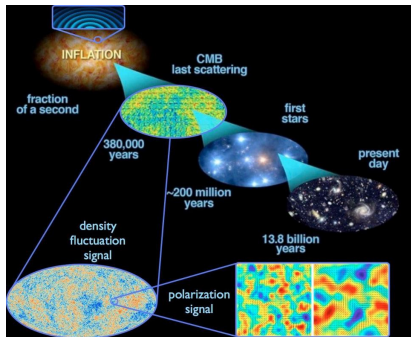
11th Iberian Gravitational Waves Meeting, June 9-11, 2021



Motivation for our analysis

Models Beyond the Standard Model (BSM) predict First Order Phase Transitions (FOPTs) in the early universe.

Energies \gg energy scale of Big Bang Nucleosynthesis and the CMB (unreachable at LHC) \Rightarrow GWs can be an alternative probe. E.g.:



- Peccei-Quinn (PQ) symmetry breaking
- High-scale Supersymmetry (SUSY) breaking

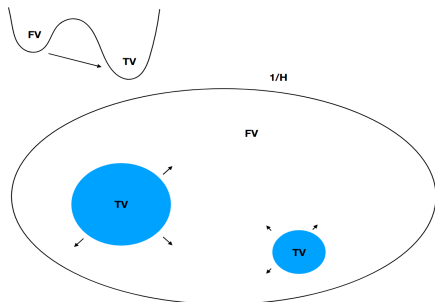
Open questions:

- Neutrino masses
- Origin of dark matter
- Inflationary models ending in a FOPT (sourced by bubble collisions)

FOPTs - Introduction

In a cosmological First Order Phase Transition (FOPT) :

- ▶ Universe goes from: metastable high energy (symmetric) phase (FV) \rightarrow stable lower energy (broken) phase (TV).
- ▶ Process: quantum or thermal nucleation of bubbles of the broken phase, separated from the surrounding unbroken phase by a wall.



These bubbles expand, collide and eventually coalesce, generating shear stresses which source gravitational waves (GWs).

FOPTs - Introduction

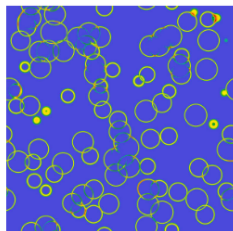
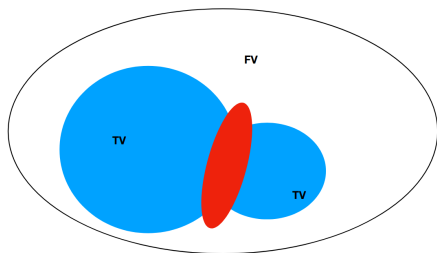


Photo retrieved from
this paper

Sources of GWs:

- ▶ Bubble collisions (BC): Ω_{coll}
- ▶ Sound waves (SW): $\Omega_{\text{sw}} \rightarrow$ Numerical simulations show that the coupling between ϕ (field) and the relativistic particles will induce SW by the expansion of the bubbles. These are the dominant GW production mechanism.
- ▶ Turbulence: $\Omega_t \rightarrow$ we will consider it negligible

Multi-baseline likelihood

We choose a Gaussian log-likelihood for a single detector pair,

$$\log p(\hat{C}_{IJ}(f) | \boldsymbol{\theta}_{\text{gw}}, \lambda) \propto -\frac{1}{2} \sum_f \frac{[\hat{C}_{IJ}(f) - \lambda \Omega_{\text{gw}}(f, \boldsymbol{\theta}_{\text{gw}})]^2}{\sigma_{IJ}^2(f)},$$

where the data from the O3 analysis is encoded in:

- ▶ $\hat{C}_{IJ}(f)$ is the cross-correlation estimator of the SGWB calculated using data from detectors I and J
- ▶ $\sigma_{IJ}^2(f)$ is the corresponding variance

The GW model we fit to the data is $\Omega_{\text{GW}}(f, \boldsymbol{\theta}_{\text{gw}})$, with parameters $\boldsymbol{\theta}_{\text{gw}}$. λ represents the calibration uncertainties of the detectors

Model Selection and comment on Schumann resonances

We use the Bayes factors (BF) to show preference for one model over another. E.g.

$$\mathcal{B}_{\text{NOISE}}^{\text{GW}} = \frac{\int d\boldsymbol{\theta}_{\text{gw}} p(\hat{C}_{IJ}(f) | \boldsymbol{\theta}_{\text{gw}}) p(\boldsymbol{\theta}_{\text{gw}})}{\mathcal{N}},$$

where \mathcal{N} is given by evaluating the log likelihood with $\Omega_{\text{GW}}(f) = 0$, and $p(\boldsymbol{\theta}_{\text{gw}})$ is the prior on the GW model parameters. In the case that $\log \mathcal{B}_N^S < 0$, there is no evidence for a signal described by the chosen model.

- ▶ There is no evidence for correlated magnetic noise in O3. Data is well described by a Gaussian stationary noise model, so we do not fit for Schumann resonances.

Searches performed

We have performed a series of searches including a Compact Binary Coalescence (CBC) background, since it is a non-negligible component of any SGWB signal. We model it as:

$$\Omega_{\text{CBC}} = \Omega_{\text{ref}} \left(\frac{f}{f_{\text{ref}}} \right)^{2/3}, \text{ where } f_{\text{ref}} = 25\text{Hz}$$

We take two different approaches in constraining the SGWB due to FOPTs. Approximated broken power law (BPL)

- ▶ BPL
- ▶ CBC + BPL

Analytical phenomenological model

- ▶ CBC + BC
- ▶ CBC + SW

Smooth Broken Power Law

We simplify and model the phase transition contribution as a smooth broken power law (BPL) function,

$$\Omega_{\text{BPL}}(f) = \Omega_* \left(\frac{f}{f_*} \right)^{n_1} \left[1 + \left(\frac{f}{f_*} \right)^\Delta \right]^{(n_2 - n_1)/\Delta}.$$

Where we fix $n_1 = 3$ by causality, $\Delta = 2$ ¹, and depending on the source of the GWs, n_2 takes the values:

- ▶ $n_2 = -1 \rightarrow$ corresponding to assuming GW sourced by BC
- ▶ $n_2 = -4 \rightarrow$ corresponding to assuming GW sourced by SW

With this, we present results for Ω_{BPL} considering as parameters: $\theta_{\text{gw}} = (\Omega_{\text{ref}}, f_*, \Omega_*)$.

¹This choice corresponds to sound waves. We present the results for this value since this choice gives more conservative upper limits.

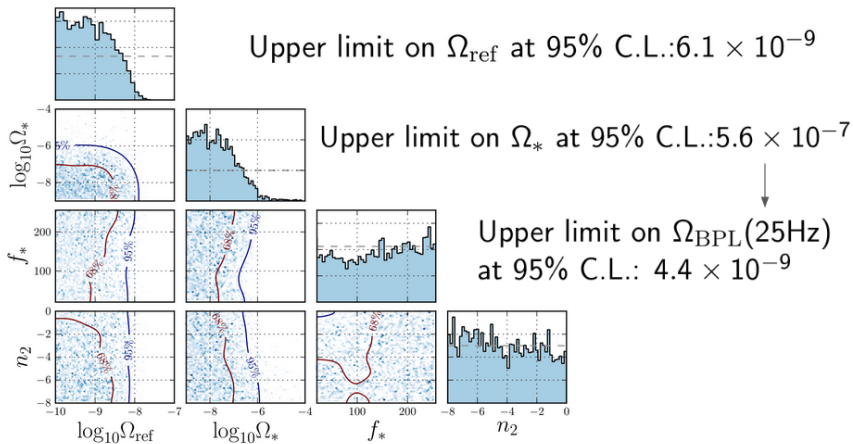
Priors used for the CBC+BPL search

$$\Omega_{\text{BPL}}(f) = \Omega_* \left(\frac{f}{f_*}\right)^{n_1} \left[1 + \left(\frac{f}{f_*}\right)^\Delta\right]^{(n_2 - n_1)/\Delta} .$$

Broken power law model	
Parameter	Prior
Ω_{ref}	LogUniform(10^{-10} , 10^{-7})
Ω_*	LogUniform(10^{-9} , 10^{-4})
f_*	Uniform(0, 256 Hz)
n_1	3
n_2	Uniform(-8,0)
Δ	2

Table 1: List of prior distributions used for all parameters from the CBC+BPL model. The narrow, informative prior on Ω_{ref} stems from the estimate of the CBC background. The peak frequency prior is uniform across the frequency range considered since we have no information about it.

BPL + CBC



Posterior distributions for the parameters of this model. $\log \mathcal{B}_N^S = -1.4$.
The UL on Ω_{ref} is consistent with the result obtained in the **search for an isotropic background**.

Upper limit on Ω_* at 95% CL

$$\Omega_{\text{BPL}}(f) = \Omega_* \left(\frac{f}{f_*}\right)^3 \left[1 + \left(\frac{f}{f_*}\right)^2\right]^{(n_2-3)/2}$$

Broken power law model			
$\Omega_*^{95\%}$			
	$f_* = 1 \text{ Hz}$	$f_* = 25 \text{ Hz}$	$f_* = 200 \text{ Hz}$
$n_2 = -1$	3.3×10^{-7}	3.5×10^{-8}	2.8×10^{-7}
$n_2 = -2$	8.3×10^{-6}	6.0×10^{-8}	3.7×10^{-7}
$n_2 = -4$	5.2×10^{-5}	1.8×10^{-7}	3.7×10^{-7}

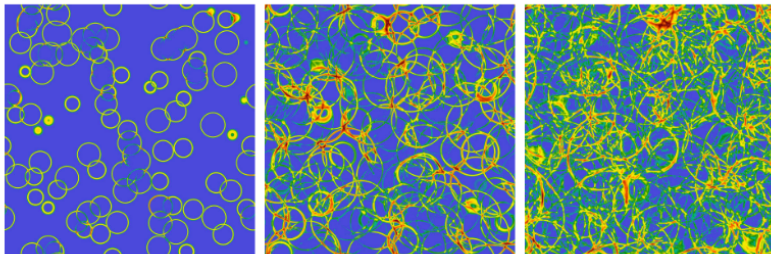
Table 2: Upper limits for the energy density amplitude, $\Omega_*^{95\%}$, in the broken power law model for fixed values of the peak frequency, f_* , and negative power law index, n_2 .

The choice of f_* is done in such a way that there is one value below the sensitivity range (1Hz), one in the sens. range (25Hz) and another one above (200Hz).

Phenomenological model parameters

The parameters to consider are the following:

- T_{pt} : temperature after the GW generation (GeV)
- v_w : bubble wall 'terminal' velocity (units of speed of light)
- α : strength of the transition
- $\frac{\beta}{H_{\text{pt}}}$, with β the inverse duration of the PT (H_{pt} =hubble rate at the time of the transition)
- $\kappa_t, \kappa_\phi, \kappa_{sw}$: 'efficiencies' of each type of signal.



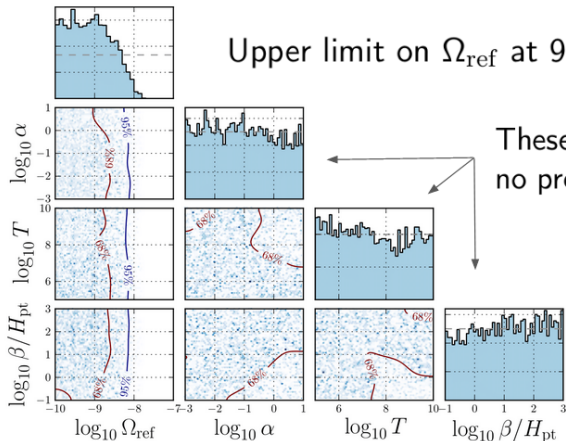
Priors used for the CBC+phenomenological model search

$$\Omega_{\text{sw}}(f)h^2 = 2.65 \times 10^{-6} \left(\frac{H_{\text{pt}}}{\beta} \right) \left(\frac{\kappa_{\text{sw}} \alpha}{1 + \alpha} \right)^2 \left(\frac{100}{g_*} \right)^{1/3} \times v_w \left(\frac{f}{f_{\text{sw}}} \right)^3 \left(\frac{7}{4 + 3(f/f_{\text{sw}})^2} \right)^{7/2} \Upsilon(\tau_{\text{sw}});$$

$$\Omega_{\phi}(f)h^2 = 1.67 \times 10^{-5} \Delta \left(\frac{H_{\text{pt}}}{\beta} \right)^2 \left(\frac{\kappa_{\phi} \alpha}{1 + \alpha} \right)^2 \times \left(\frac{100}{g_*} \right)^{1/3} S_{\text{env}}(f)$$

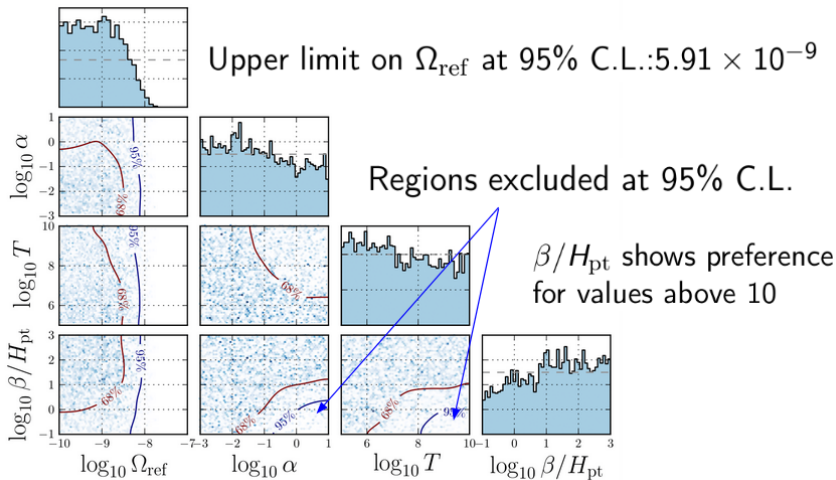
Phenomenological model	
Parameter	Prior
Ω_{ref}	LogUniform(10^{-10} , 10^{-7})
α	LogUniform (10^{-3} , 10)
β/H_{pt}	LogUniform (10^{-1} , 10^3)
T_{pt}	LogUniform (10^5 , 10^{10} GeV)
v_w	1
κ_{ϕ}	1
κ_{sw}	$f(\alpha, v_w) \in [0.1 - 0.9]$

SW + CBC: $\theta_{\text{gw}} = (\Omega_{\text{ref}}, \alpha, \beta/H_{\text{pt}}, T_{\text{pt}})$,
 $v_w = 1, \kappa_{\text{SW}} = f(\alpha, v_w)$



Posterior distributions for the parameters of this model. $\log \mathcal{B}_N^S = -0.661$

BC + CBC: $\theta_{\text{gw}} = (\Omega_{\text{ref}}, \alpha, \beta/H_{\text{pt}}, T_{\text{pt}})$, $v_w = \kappa_\phi = 1$



Posterior distributions for the parameters of this model. $\log \mathcal{B}_N^S = -0.729$

Upper limit on Ω_{coll} at 95% CL

From running the Bayesian search with delta priors on T_{pt} and β/H_{pt} we obtain the UL on α and then compute the UL on Ω_{coll} , keeping in mind that $h\Omega_{\text{coll}} \propto \alpha^2/(1 + \alpha)^2$

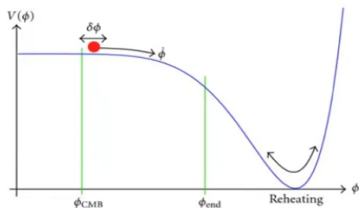
Phenomenological model (bubble collisions)				
$\Omega_{\text{coll}}^{95\%}$ (25 Hz), $v_w = \kappa_\phi = 1$				
β/H_{pt}	$T_{\text{pt}} = 10^7$ GeV	$T_{\text{pt}} = 10^8$ GeV	$T_{\text{pt}} = 10^9$ GeV	$T_{\text{pt}} = 10^{10}$ GeV
0.1	9.2×10^{-9}	8.8×10^{-9}	1.0×10^{-8}	7.1×10^{-9}
1	1.0×10^{-8}	8.4×10^{-9}	5.0×10^{-9}	-
10	4.0×10^{-9}	6.3×10^{-9}	-	-

For all these searches, the *UL* at 95% CL on Ω_{ref} is between 5.3×10^{-9} to 6.1×10^{-9} .

Formation of primordial Black Holes (PBH) - Ongoing work

PBH formation

- ▶ PBHs were formed in the early radiation-dominated era
- ▶ Source: highly over-dense region that would gravitationally collapse into a black hole, known as primordial (PBH). Said otherwise, PBHs are the product of the collapse of large density perturbations.



- ▶ These density perturbations could have been formed during inflation (due to quantum fluctuations of ϕ)
- ▶ In the case of "slow roll" inflation, the production would be from ϕ_{CMB} to ϕ_{end}
- ▶ The collapse of δ takes place precisely when they reenter the horizon

Production of GWs

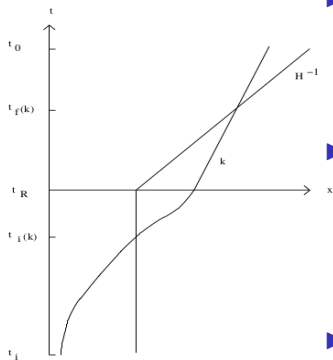


Figure 1: Scale re-entering the horizon

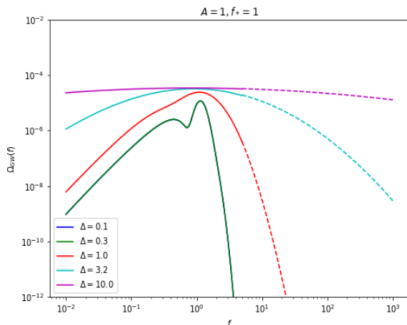
- ▶ Inflationary period $t \in [t_i, t_R]$
- ▶ During inflation, the Hubble radius H^{-1} is constant in spatial coordinates, whereas it increases linearly in time after t_R .
- ▶ The physical length corresponding to a fixed comoving length scale (k) increases exponentially during inflation but increases less fast than the Hubble radius after t_R .
- ▶ This leads k to re-enter the horizon, which is when GWs are generated (at the same epoch as the PBH formation)

The SIGW spectrum: $\Omega_{GW}(f)$

Model independent search: we consider a log-normal shape of the spectrum for the peak generated in single field inflation

$$\mathcal{P}_\zeta(f) = A \exp \left[-\frac{\ln^2(f/f_*)}{\Delta^2} \right] \quad (1)$$

where f_* is the peak frequency, A the amplitude of the spectrum and Δ its width. The energy density spectrum for scalar induced gravitational waves (SIGW) is retrieved from [this paper](#).



Conclusions

- ▶ Many models BSM predict FOPTs in the early universe. For $T_{\text{pt}} \in [10^7, 10^9]$ GeV the produced SGWB is within the frequency range of Ad-LIGO and AdV \Rightarrow we have performed a Bayesian search and model selection study using O3 data. All of these results are now published in [Phys. Rev. Lett. 126, 151301 – Published 16 April 2021](#)
- ▶ We have followed the same analysis assuming the stochastic background is mainly sourced by GWs from CBCs and the formation of primordial black holes. We are soon going to publish these results.
- ▶ Even though no SGWB signal was detected, we could place ULs over some parameters of the FOPT models (at the reference frequency of 25Hz)
- ▶ The results indicate the relevance of the LIGO-Virgo GW data to place constraints on new phenomena related to strong FOPTs at large T in the early universe as well as on the formation of PBHs.

We would like to thank Pat Meyers for allowing us to use his code and Alberto Mariotti for his useful comments.

Functional form of the GWs from bubble collisions

$$\Omega_{\phi}(f)h^2 = 1.67 \times 10^{-5} \Delta \left(\frac{H_{\text{pt}}}{\beta} \right)^2 \left(\frac{\kappa_{\phi} \alpha}{1+\alpha} \right)^2 \times \left(\frac{100}{g_*} \right)^{1/3} S_{\text{env}}(f); \Delta(v_w) = 0.48 v_w^3 / (1 + 5.3 v_w^2 + 5 v_w^4)$$

$$S_{\text{env}} = 1 / (c_l \tilde{f}^{-3} + (1 - c_l - c_h) \tilde{f}^{-1} + c_h \tilde{f}), c_l = 0.064, c_h = 0.48, \tilde{f} = f / f_{\text{env}};$$

$$f_{\text{env}} = 16.5 \left(\frac{f_{\text{bc}}}{\beta} \right) \left(\frac{\beta}{H_{\text{pt}}} \right) \left(\frac{T_{\text{pt}}}{100 \text{ GeV}} \right) \left(\frac{g_*}{100} \right)^{1/6} \mu\text{Hz}; f_{\text{bc}} = 0.35 \beta / (1 + 0.069 v_w + 0.69 v_w^4)$$

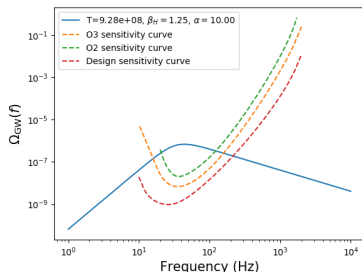
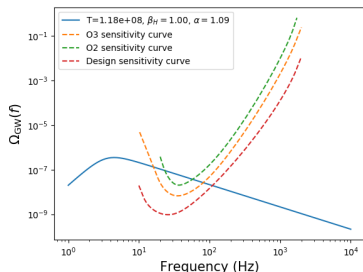


Figure 2: In red \rightarrow O3 sensitivity curve (that with respect to which we have compared our models). In yellow \rightarrow that expected for Ad-LIGO +.

Functional form of the GWs from sound waves

$$\Omega_{\text{SW}}(f)h^2 = 2.65 \times 10^{-6} \left(\frac{H_{\text{pt}}}{\beta} \right) \left(\frac{\kappa_{\text{SW}} \alpha}{1 + \alpha} \right)^2 \left(\frac{100}{g_*} \right)^{1/3} \times v_{\text{w}} \left(\frac{f}{f_{\text{SW}}} \right)^3 \left(\frac{7}{4 + 3(f/f_{\text{SW}})^2} \right)^{7/2} \Upsilon(\tau_{\text{SW}});$$

$$f_{\text{SW}} = 19 \frac{1}{v_{\text{w}}} \left(\frac{\beta}{H_{\text{pt}}} \right) \left(\frac{T_{\text{pt}}}{100 \text{ GeV}} \right) \left(\frac{g_*}{100} \right)^{1/6} \mu\text{Hz}$$

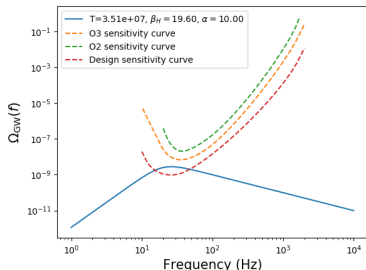
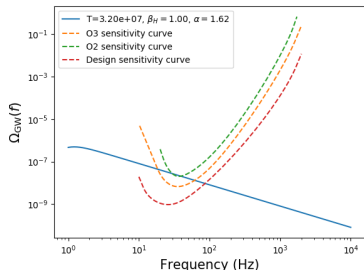


Figure 3: In blue we have Ω_{GW} for a FOPT.

Choice of n_2

- ▶ The value of the rising spectral index in the broken power law approximation of a FOPT signal, $n_1 = 3$, is fixed due to causality.
- ▶ However, n_2 parameter for the GW contributions changes with every new numerical simulation.
- ▶ We test the robustness of our upper limits w.r.t. n_2 in the case of Ω_{coll} , where most recent searches show $n_2 = -2.3$

Prior	$\frac{\Delta\Omega_*}{\Omega_*}, n_2=-1$	$\frac{\Delta\Omega_*}{\Omega_*}, n_2=-2.3$
LogUniform($10^{-5}, 10^{-2}$)	0.2%	0.2%
LogUniform($10^{-6}, 10^{-2}$)	2.5%	3.0%
LogUniform($10^{-7}, 10^{-2}$)	7.5%	8.3%

Table 3: Percentage uncertainty of Ω_{coll} upper limit for searches with different n_2 on O3a data. Upper limit robust with respect to n_2 since percentage uncertainties for the two cases are within 1%.

Searches assuming a CBC+SW model and different v_w

Bubble wall velocity (v_w)	Log Bayes factor ($\log \mathcal{B}_N^S$)	UL at 95% CL on Ω_{ref}
0.7	-0.607	5.93×10^{-9}
0.8	-0.597	5.77×10^{-9}
0.9	-0.668	5.84×10^{-9}

Table 4: For different v_w , we compute the upper limit at 95% CL on Ω_{ref} for a reference frequency of 25Hz and the Bayes factors of signal vs noise when considering a CBC+SW model.

The models with reduced velocities lead to lower Ω_{SW} , and with no 95%CL exclusions in the considered parameter space. There is no difference in the UL on Ω_{ref} as v_w is varied, so in the paper we have decided to state as main results those corresponding to a search with $v_w = 1$.

Reference UL on Ω_{ref} at 95% CL

We perform a simplified Bayesian analysis considering contributions from unresolved CBC sources plus an unmodelled generic term with a log-uniform prior in the range: $10^{-17} - 10^{-5}$:

$$\Omega_{\text{CBC}} + \Omega_{\text{extra contributions to the SGWB}}$$

From this search we found an UL at 95% CL in:

- ▶ $\Omega_{\text{ref}} : 6.6 \cdot 10^{-9}$
- ▶ $\Omega_{\text{extra contributions to the SGWB}} : 3.3 \cdot 10^{-9}$

In this case, the Bayes factor of model vs noise is $\log \mathcal{B}_N^S = -0.6$, i.e.: it shows no evidence for a SGWB

Efficiency associated to sound waves

The parameters used in this Eq. are in the next slide

$$\kappa_V(\alpha, v_W) = \begin{cases} 0, & \text{if } v_W < 1 - (3\alpha) \\ \frac{c_s^{11/5} \kappa_1 \kappa_2}{(c_s^{11/5} - v_W^{11/5}) \kappa_2 + v_W c_s^{6/5} \kappa_1}, & \text{if } v_W \leq c_s \\ \frac{\kappa_2 + dk(-c_s + v_W) + [-\kappa_2 + \kappa_{JD} - dk(-c_s + v_J)] \times (-c_s + v_J)^{-3} (-c_s + v_W)^3}{\kappa_{JD} \kappa_{vW1} (-1 + v_J)^3 v_J^{2.5} v_W^{-2.5} \times 1}, & \text{if } c_s < v_W < v_J \\ \frac{1}{\kappa_{JD} v_J^{2.5} [(-1 + v_J)^3 - (-1 + v_W)^3] + \kappa_{vW1} (-1 + v_W)^3}, & \text{if } v_W \geq v_J \end{cases}$$

Efficiency associated to sound waves - Parameters

$$c_s = 1/\sqrt{3} \quad (2)$$

$$v_J = \frac{\sqrt{2/3\alpha + \alpha^2} + c_s}{1 + \alpha} \quad (3)$$

$$dk = -0.9 \log \frac{\sqrt{\alpha}}{1 + \sqrt{\alpha}} \quad (4)$$

$$\kappa_1 = 6.9 \cdot \alpha \cdot v_w^{1.2} \frac{1}{1.36 + \alpha - 0.037\sqrt{\alpha}} \quad (5)$$

$$\kappa_2 = \alpha^{0.4} \frac{1}{0.017 + (0.997 + \alpha)^{0.4}} \quad (6)$$

$$\kappa_{JD} = \alpha^{0.5} \frac{1}{0.135 + (0.98 + \alpha)^{0.5}} \quad (7)$$

$$\kappa_{vw1} = \alpha \frac{1}{0.73 + \alpha + 0.083\sqrt{\alpha}} \quad (8)$$

$F(x, y)$

$$F(x, y) = \frac{288(x^2 + y^2 - 6)^2(x^2 - 1)^2(y^2 - 1)^2}{(x - y)^8(x + y)^8} \times \left[\left(x^2 - y^2 + \frac{x^2 + y^2 - 6}{2} \ln \left| \frac{y^2 - 3}{x^2 - 3} \right| \right)^2 + \frac{\pi^2}{4} (x^2 + y^2 - 6)^2 \theta(y - \sqrt{3}) \right]$$

Where $\theta(y - \sqrt{3})$ is the Heaviside function and a graphic representation is:

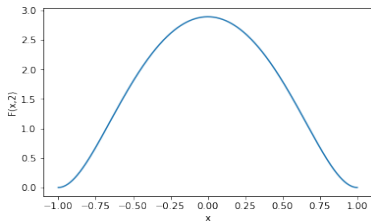


Figure 4: Fixed $y=2$

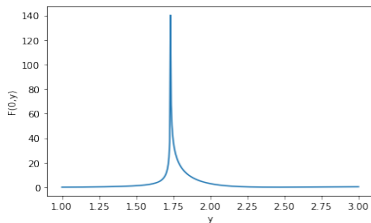


Figure 5: Fixed $x=0$